ACS OMEGA

http://pubs.acs.org/journal/acsodf

Article

Chemical Speciation and Leaching Behavior of Hazardous Trace Elements in Coal Combustion Products from Coal-Fired Power Stations in China

Patricia Córdoba,* Baoqing Li, Jing Li, Xinguo Zhuang, and Xavier Querol

Cite This: *ACS Omega* 2022, 7, 14697−14711

Read Online

ACCESS | Metrics & More | Article Recommendations | Supporting Information

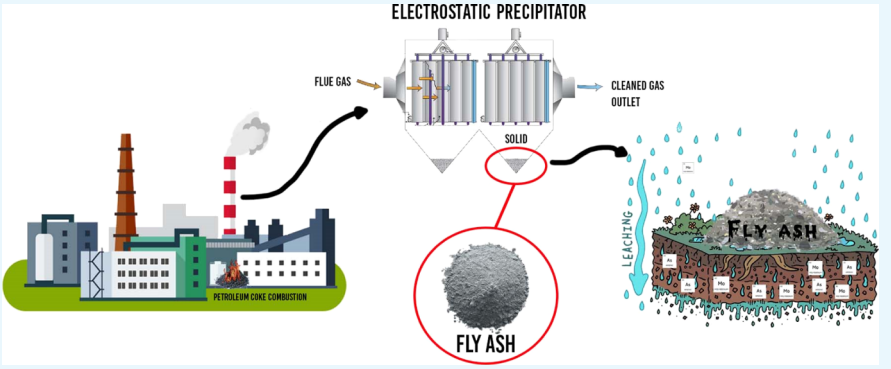

ABSTRACT: This paper reports on the chemical speciation and leaching behavior of a selected group of hazardous trace pollutants in lignite and lignite-petcoke blend co-combustion products from three power stations in China. The evaluation of speciation results showed that, during combustion, oxidizable elements, mainly As and Mo, bound to organic matter and sulfides in coals were mostly transferred to easily water-soluble forms or to slightly acidic states in the ashes. This manner was the most readily bioavailable condition for such an environment. The evaluation of the leaching results shows that the use of petroleum coke as co-fuel has an impact on the ash composition and on the leaching behavior of some inorganic trace pollutants such as Mo and V. The leaching results compared to the European waste acceptance criteria for landfills reveal that the Mo and As' leaching yield brand the coal combustion products as materials that necessitate preventative measures to reduce their potential leaching. Future work will be focused on the application of our novel chemical stabilization method to these coal ashes to reduce the mobility of elements such as Mo and As, and other potentially leachable elements, and on the use of the resulting ash with aggregate products as a substitute for concrete production.

1. INTRODUCTION

Despite the global regulations and financial incentives to switch to renewable energy, it has not been until the pandemic outbreak that electricity use and the industrial production of coal have started to fall worldwide. In the European Union (EU), coal demand fell by more than 20% due to the attenuation of electricity demand during lockdowns. However, the low gas prices and, most importantly, the increasing renewable output[1] also led to such a fall worldwide.

In the United States (US), coal's share fell below 20% in the energy mix for the first time since the widespread development of coal-fired electricity.[1] This significant drop was driven by the expansion of renewables along with the decrease in the price of natural gas. However, the vast decline in electricity consumption during lockdowns pushed coal out of the energy mix. In China, the world's largest coal consumer and producer, coal consumption fell by 8% in Q1 2020 compared to 2019 and coal power generation dropped by approximately 9%[1] as the economy contracted by 6.8%. However, the forecast by BP[2] on Global Energy Outlook predicts constant coal consumption for power generation for the next 2 decades in China. Furthermore, after the COVID lockdown, China proposed to increase fossil fuel consumption instead of renewable energy, including an approximately $25 billion investment in coal power plants and significantly more on mining and processing.[3]

The environmental impact of coal power generation, counting the use of co-fuels such as petroleum coke, includes large emissions of carbon dioxide (CO_2), the main greenhouse

Received: December 28, 2021
Accepted: April 7, 2022
Published: April 21, 2022

https://doi.org/10.1021/acsomega.1c07326
ACS Omega 2022, 7, 14697−14711

gas, air quality pollutants [e.g., NO_x and SO_2, primary and secondary particulate matter (PM)], and heavy metals. It also generates millions of tons of coal combustion products (CCPs).

Most of the petroleum coke used by emerging economies in Asia, such as in China and India, to generate electricity in power plants is a cause for concern because high petroleum coke combustion may increase sulfur dioxide (SO_2) emissions.[4] Co-firing petroleum coke may also modify the chemical environment of chlorine (Cl)[5,6] because of the resultant high concentrations of hydrochloric acid (HCl) in the gaseous stream. For numerous elements, an increase in the HCl concentration favors the formation of gaseous species, whereas an increase in the concentration of SO_2 in the gas composition enhances the formation of sulfate-condensed species.[7] The organic affinity of elements such as molybdenum (Mo), vanadium (V), and nickel (Ni) in petroleum cokes favors their volatility during pulverized coal combustion (PCC) and later condensation into the finest fly ash (FA) particles.[8,9] Indeed, previous research[10] showed that a fuel blend with 30% petroleum coke, in comparison to a fuel blend with 4% petroleum coke, increased the volatility of Cl, fluorine (F), selenium (Se), sulfur (S), thallium (Tl), tin (Sn), boron (B), and mercury (Hg), and the enrichment of V, Ni, and Mo in FA.

Major CCPs include FA, bottom ash (BA), boiler slag (BS), fluidized bed combustion (FBC) ash, and products from wet or dry flue gas desulfurization (FGD). FA is a fine powder captured in particulate control devices from the flue gases of boilers fired with coal or lignite from 1100 to 1400 °C in PCC plants.[11] The FA is composed of spherical high Si−Al−Ca−K−Fe−Ti−Mg vitreous particles with Fe oxides and Al−Si species, and irregular unburned coal and ash particles.[12] The FBC ash is produced in FBC boilers where coal combustion and FGD occur simultaneously at temperatures of 800−900 °C. The FBC ash is, therefore, rich in lime (CaO) and S. The BA is the coarse fraction of ashes normally removed from the bottom of dry boilers, while the BS is a vitreous grained material derived from coal combustion in boilers at temperatures of 1500−1700 °C, followed by wet ash removal from wet bottom furnaces.

In 2010, the first global compilation of the worldwide production of CCPs, disclosed that 780 million metric tonnes (Mt)[13] of CCPs were manufactured. In 2017, an update[14] indicated production rose to 1.1 Gt. The Annual Production and Utilization Report revealed rates of CCPs generated by country in 2016, where the largest CCP-producing countries were China (565 Mt), India (197 Mt), Europe (total production of 140 Mt considered for EU15), and the US (104 Mt). The total production estimate for 2016 totaled nearly 1.2 Gt.

Since the 1950s, FA has served as an additive in the production of cement and concrete, and it is the most successful utilization technique worldwide.[15] In addition, about 9% of the production of coal fly ash (CFA) is in emerging applications such as high-end building materials (ceramics), element extraction, and agricultural melioration.[16] The official FA utilization rate in China has reached 70% of the production,[6] primarily through the cement industry (44%), and the manufacture of concrete walling products (28%). The usual final fate for the unused FA (i.e., 150−180 Mt from 565 Mt of total production) is disposal in lagoons, settling ponds, or landfills.[17]

The content of trace elements in FA and FBC ashes is an important factor to monitor because a high concentration of CaO in FA causes an alkalinity in pH in their leachates, which favors the mobility of elements in their oxy-anionic form. Therefore, such properties may lead to environmental leaching problems that ultimately may reduce the reuse options of this solid residue. The EU's cutoff criteria[18] for the leaching of several elements and procedures for waste admission and landfills were developed out of these concerns. These standards, which are imperative for landfill management purposes, specify the limits within which certain substances must comply. They also define how to analyze them in the leachate form within a given waste by applying the EN-12457-4 leaching test. However, compliance with the limit of trace elements leaching in CCPs may be unaffordable not only due to the implementation cost but also because of incomplete knowledge of the partition and speciation in CCPs.

This work aims to determine (i) the elemental composition and chemical speciation of select hazardous trace elements (HTEs) in lignites and lignite-petcoke blends used to feed a PCC and two FBC power stations in China; (ii) the morphological features and elemental composition of FA from the PCC power station and ashes from the two FBC power stations, including the chemical speciation of selected HTEs; (iii) enrichment factors and partitioning of selected HTEs across output streams during combustion in three power stations; (iv) the level of risk of the labile (mobile) fraction of HTEs on the environment and the leachability patterns of HTEs in FA and FBC ashes for subsequent remediation actions; and (v) the effect of using petcoke as co-fuel on the abovementioned environmental parameters.

2. MATERIALS AND METHODS

2.1. Power Stations. Power station 1 (PS1) is a PCC power plant fed with lignite coal and equipped with selective catalyst reduction, which combines the flue gases with precise amounts of ammonia (NH_3) over catalysts, followed by a cold-side electrostatic precipitator (ESP, 80−220 °C) and an NH_3-FGD system. Power station 2 (PS2) is an FBC plant fed with a blend of lignite coal and petroleum coke and equipped with bag filters (BFs) and a wet limestone-based FGD system. Limestone at PS2 is used to both create the fluidized bed in the combustion unit and as an alkaline sorbent for the desulfurization process. Power station 3 (PS3) is also an FBC plant, fed with lignite coal and equipped with BFs and a wet limestone-based FGD system. Similarly to PS2, limestone at PS3 is used to both create the fluidized bed in the combustion unit and as an alkaline sorbent for the desulfurization process.

2.2. Sample Collection. The sampling procedure was based on collecting samples from all the ingoing and outgoing flows to represent the specific burning process at the power station. Input and output flows were sampled in the coal combustion in stable operational conditions with the objective of achieving representative samples during the sampling campaign. The sampling points were selected together with the operators and staff of the power plants to ensure the safety of the sampling personnel and to prevent interruptions in process operations.

The coal-fired power station samples were collected at 100% maximum capacity in April 2019. A total of three solid streams including lignite coal, BS, and FA were sampled at PS1. Six solid streams consisting of lignite coal, petroleum coke, feed

https://doi.org/10.1021/acsomega.1c07326
ACS Omega 2022, 7, 14697−14711

Table 1. Description of the BCR Sequential Extraction Procedure Used for HTEs Speciation

fraction	BCR sequential extraction procedure		
F1	0.11 M CH_3COOH (40 mL)	16 h at laboratory temperature	exchangeable hazardous elements (e.g., carbonates and highly water-soluble and/or under acidic conditions)
F2	$HONH_2HCl$ (40 mL)	16 h at laboratory temperature	hazardous elements (e.g., bound to either Fe and/or Mn oxyhydroxides)
F3	8.8 M H_2O_2 (10 mL) + 1 M $NH_4C_2H_3O_2$ (50 mL)	1 h at laboratory temperature and 1 h at 85 °C, +1 h at 85 °C, +16 h at laboratory temperature	hazardous elements (e.g., associated with both organic matter and sulfides)
F4	$HNO_3/HF/HClO_4$	two-step acid digestion method devised by Querol et al.	hazardous elements (e.g., associated with crystalline and amorphous phases)

fuel blend, limestone (used for the FBC), BA, and FBC ash were sampled at PS2. Lignite coal, BA, and FBC ash were sampled at PS3.

Individual lignite coals at PS1, lignite coal, petroleum coke, and feed fuel blend at PS2, and lignite coals at PS3 were collected from the feeders. Samples of the feed fuel blends were collected using an automatic sampler in periods of 6 min. BS and BA samples were collected from the boiler once it was discharged into the vessel. The solid samples, composed of lignite coals, feed fuel blend, BS, and BA, were homogenized, riffled, and divided into subsamples of 5 kg. FAs were sampled from the ESP using automatic samplers and BFs, respectively. FA samples were then mixed, homogenized, riffled, and divided into subsamples of 5 kg.

From each subsample, a solid sample of 1 kg was air dried at a constant 60 °C for the analysis of major, minor, and trace elements, including the leaching tests, whereas a duplicate of each solid sample (1 kg) was only air dried for the analysis of Hg. Samples were held in polyvinyl chloride bottles for subsequent analyses at IDÆA-CSIC.

In this article, the term PS1 FA is used to designate the FA generated at PS1, which functions under PCC conditions, while PS2 ash and PS3 ash are used to designate the ash generated at PS2 and PS3, respectively, both functioning under FBC conditions. Under the same criteria, PS1 BS is used to designate the BS generated at PS1. PS2 BA and PS3 BA are used to denote the BA generated at PS2 and PS3, respectively.

2.3. Physical−Chemical Analyses. *2.3.1. Bulk Analysis.* A portion of the dried solid samples was acid digested in duplicate using a specific two-step method devised by Querol et al. (1993) to retain volatile elements. Several reagent blanks, the standard reference materials NIST SRM 1633b (FA) and SARM 19 (South African coal, Council for Mineral Technology) helped ascertain the accuracy of the analytical and digestion methods. The concentrations of major elements in the acid digests were determined using inductively coupled plasma (ICP) atomic emission spectrometry (Iris Advantage Radial ER/S device from Thermo Jarrell-Ash). Trace elements were analyzed via ICP mass spectrometry (ICP−MS, X-SERIES II Thermo Fisher Scientific, Thermo Fisher Scientific, Waltham, Massachusetts, EEUU) equipped with a helium gas reaction/collision cell to remove spectral interferences. A 10 μg/L In was used for the ICP−MS analysis as the internal standard to monitor, correct short- and long-term fluctuations in the signal, and amend the effects of unspecified matrices.

2.3.2. Mineralogical and Morphological Characterization. Powder X-ray diffraction (XRD) data for mineralogical analyses in fuels and CCPs were collected using a Bruker D8 A25 Advance $\theta-\theta$ diffractometer, with Cu Kα_1 radiation, Bragg−Brentano geometry, and a position-sensitive LynxEyeXE detector. The diffractograms were obtained at 40 kV and 40 mA, scanning from 4 to 60° of 2θ with a step size of 0.019° and a counting time of 0.1 s/step while maintaining the sample in rotation (15/min). The crystalline phase identification was conducted using an EVA software package by Bruker.

The particle resolved composition and morphology of FA were investigated using a field emission scanning electron microscope JEOL JSM-7001F with secondary and retro-dispersed electron detectors and Polaron critical point dryers, equipped with energy-dispersive X-ray spectroscopy (EDX).

A Horiba SA-9600 was used to determine the specific surface area (m^2/g) of the FA and FBC ash samples based on the Brunauer−Emmett−Teller (BET) theory. This technique uses the flowing gas method, which determines the quantity of a gas (e.g., nitrogen/helium mixture) that adsorbs as a monomolecular layer on the sample.

2.4. Enrichment Factors and Partitioning of Elements Across the Output Stream. Total enrichment factors (TEFs) were calculated to determine the fate of elements during pulverized and fluidized coal combustion in the three power stations. To this end, enrichment factors in FA ($EF_{FA/FBC\ ash}$), BS (EF_{BS}), and BA (EF_{BA}) were calculated by normalizing the concentration of a given element with respect to a nonvolatile element (e.g., Al) and their concentrations in the feed fuel blend as per in eq 1 below.

$$EF_x = ([C]_X / [Al]_X)/([C]_{FC}/[Al]_{FC}) \quad (1)$$

$[C]_X$ and $[C]_{FC}$ are the concentrations of a given element in the FA, BS/BA, and in the feed coal or feed fuel blend, respectively. $[Al]_X$ and $[Al]_{FC}$ are the corresponding Al concentrations in the FA, BS/BA, and feed coal or feed fuel blend. The TEF is then calculated as per eq 2.[19]

$$TEF = (EF_{\frac{FA}{FBC}ash} \times A) + (EF_{BS/BA} \times B) \quad (2)$$

A and B are the production proportion of the FA (90%) and BS (10%) at PS1 and FA (75%) and BA (25%) at PS2 and PS3, respectively. Although TEF ≈ 1 is reasonably expected for a range of elements, TEF < 1 for an element suggests it is primarily emitted in the gaseous form(s).

2.5. Chemical Speciation of HTEs. The four-step sequential extraction method proposed by the European Bureau of Reference (BCR)[20] was used to investigate the chemical speciation of the selected hazardous elements (i.e., Cr, Ni, Zn, As, Mo, and Pb) in the PS1 and PS3 lignite coals and in the PS2 feed fuel blend (lignite + petroleum coke). They serve as the source of trace elements in the PS2, FA and FBC ash, and in the BS and/or BA from each power station.

The BCR sequential extraction procedure[20] involves the fractionation of the total content of a given metal into four solution fractions (Table 1). The first fraction (F1) corresponds to the exchangeable hazardous elements related

https://doi.org/10.1021/acsomega.1c07326
ACS Omega 2022, 7, 14697−14711

Table 2. Average Concentration of Major, Minor, and Trace Elements in the PS1 LC, PS2 LC, PS2 PC, PS2 FB, and PS3 LC[a]

%	PS1 LC	PS2-PC	PS2-LC	PS2-FB	PS3-LC
C	29	81	33	3.0	36
N	1.1	0.9	1.4	0.9	0.8
H	2.5	3.0	3.2	2.4	1.2
Al	11	0.04	9.3	11	3.4
Ca	1.3	0.1	0.7	0.9	1.5
Fe	3.8	0.02	1.8	2.6	2.4
K	1.3	0.1	1.1	1.7	1.1
Mg	1.0	0.1	0.5	0.4	0.4
Na	0.3	0.02	0.2	0.2	0.2
P	0.03	0.001	0.04	0.2	0.1
S	2.0	8.3	2.1	2.0	1.5
mg/kg	PS1 LC	PS2-PC	PS2-LC	PS2-FB	PS3-LC
Cl	1030	1008	763	1042	537
Hg	0.2	0.003	0.3	0.2	0.2
Li	95	<dl	67	91	39
Be	1.9	<dl	3.0	3.1	1.4
B	298	31	101	176	<dl
Sc	21	<dl	11	19	9.2
Ti	3530	5.4	2104	3282	1900
V	121	435	115	205	107
Cr	87	0.3	62	78	51
Mn	141	1.9	52	115	251
Co	12	<dl	8.6	10	5.8
Ni	38	203	33	65	33
Cu	47	4	29	52	20
Zn	116	16	67	103	49
Ga	18	<dl	25	21	12
Ge	7.5	<dl	3.3	4.0	3.4
As	8.6	<dl	6.8	17	5.5
Se	3.7	<dl	1.8	4.4	2.6

mg/kg	PS1 LC	PS2-PC	PS2-LC	PS2-FB	PS3-LC
Rb	173	<dl	154	150	83
Sr	85	1.5	79	177	57
Y	23	<dl	12	18	11
Zr	139	0.9	87	146	48
Nb	9.5	<dl	7.2	11	4.9
Mo	2.5	6.3	1.1	4.9	1.0
Sn	3.4	<dl	2.0	3.4	1.2
Sb	16	<dl	17	19	15
Cs	23	<dl	12	22	9.9
Ba	389	1.9	426	455	236
La	43	<dl	26	34	17
Ce	65	<dl	53	75	23
Pr	8.3	<dl	4.8	7.3	4.2
Nd	28	<dl	21	29	12
Sm	6.7	<dl	5.0	6.2	3.1
Eu	1.2	<dl	1.3	1.0	0.9
Gd	4.4	<dl	3.7	4.4	2.3
Dy	3.7	<dl	<dl	<dl	2.2
Er	2.5	<dl	3.0	4.1	1.4
Yb	1.9	<dl	0.8	1.2	1.2
Hf	3.2	<dl	2.9	2.5	1.4
Ta	1.2	<dl	<dl	<dl	<dl
W	3.4	<dl	2.9	2.8	3.7
Tl	1.3	<dl	<dl	<dl	<dl
Pb	38	<dl	29	40	16
Th	12	<dl	12	15	6.2
U	6.4	<dl	6.0	9.2	4.9

[a]LC: lignite coal; PC: petroleum coke; and FB: feed fuel blend.

to carbonates and those highly water-soluble and/or under acidic (medium to low) conditions. This fraction, thus, is characterized by the presence of the most mobile elements and should be considered a potential threat to the environment.

The second fraction (F2) corresponds to the hazardous elements bound to either Fe and/or Mn oxyhydroxides that might be released depending on the redox conditions in the environment. The third fraction (F3) denotes hazardous elements associated with both organic matter and sulfides, making them liable to leach out under oxidizing conditions. The sum of these three fractions represents the total metal content associated with the mobile phase.

The fourth fraction (F4) relates to the hazardous elements associated with crystalline and amorphous phases. Harmful elements in this fraction are unlikely to be released unless exposed to extreme weathering conditions. The extraction procedure of this fraction is based on the two-step acid (HNO_3/HF/$HClO_4$) digestion method devised by Querol et al.[21]

The concentrations of hazardous elements in each fraction were determined by ICP−MS operating with a collision cell to remove spectral interferences.

The accuracy of the extraction method was performed by comparing the sum of the four fractions of the sequential extraction to the results obtained from the total digestion per the recovery percentage, which is displayed below.

$$\text{Recovery (\%)} = \frac{\text{fraction 1} + \text{fraction 2} + \text{fraction 3} + \text{fraction 4}}{\text{total digestion}} \times 100$$

2.6. Risk Assessment Code. In this study, the risk assessment code (RAC) is used to evaluate the level of risk of the labile (mobile) fraction of HTEs on the environment.[22] Based on the ratio of easily soluble fraction (i.e., water/acid-soluble and exchangeable fraction), the HTEs in the labile fraction (F1) were considered no risk when RAC is <1%, low risk 1−10%, medium risk 11−30%, high risk 31−50%, and remarkably high risk >50%.

2.7. Leaching Behavior of HTEs in the FA and FBC Ashes. Leaching tests evaluated the leachability patterns of the selected HTEs with regard to their future disposal in landfills. The analyses referred to the EN12457-4 (14) standard set out by the EU (2003/33/EC) and were applied to the PS1 FA and PS2 and PS3 ashes. The procedure consisted of a single-batch leaching test that used Milli-Q water as the leaching agent at a liquid-to-solid ratio of 10 L/kg and 24 h of agitation time in an orbital shaker (300 rpm). Duplicated samples and blanks were prepared similarly. The leachates were filtered through 0.45 μm filters and divided into two aliquots inside high-density polyethylene bottles. One aliquot was used to determine pH and major anions, while the other was acidified with 1% HNO_3 for further analysis of major and trace metals using ICP−MS.

https://doi.org/10.1021/acsomega.1c07326
ACS Omega 2022, 7, 14697−14711

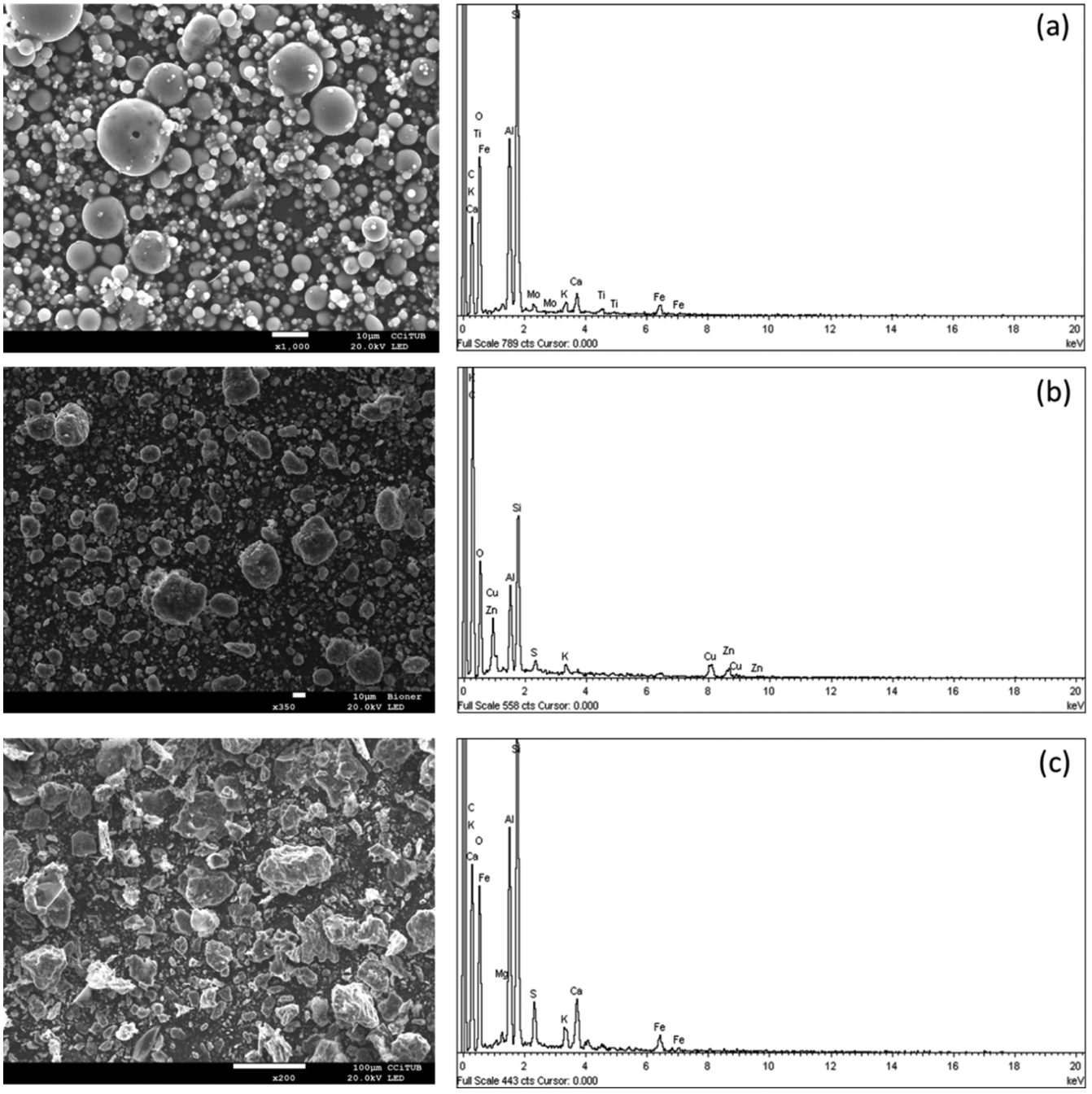

Figure 1. SEM photomicrographs and EDX analysis of the (a) PS1 FA, (b) PS2 ash, and (c) PS3 ash.

3. RESULTS AND DISCUSSION

Elemental analysis (%), ash (%) and moisture (%) content, and concentration (mg/kg) of major, minor, and trace elements in samples with their corresponding replicates, including statistics, are provided in the Supporting Information (TS1−TS5). The following discussion is based on average results.

3.1. Fuel Characterization. The lignite coal from PS1 presented a high-ash yield (40−45%) with relatively high S (2.0%) and low N (1.1%), as shown in Table 2, and demonstrated remarkable enrichment in Cl (1030 mg/kg), Ti (3530 mg/kg), Ba (421 mg/kg), V (121 mg/kg), Rb (173 mg/kg), and Cr (87 mg/kg) compared to the average concentrations in coal in China[23] and worldwide.[24]

The lignite coal from PS2 showed a similar chemical composition to that of PS1, which is again shown in Table 1, with relatively lower concentrations of S (2.1%) and As (6.8 mg/kg). The petroleum coke had a distinctive chemical composition characterized by high S (8.3%) and C (81%) contents and a 1.4−5.7-fold enrichment in Ni (203 mg/kg) and Mo (6.3 mg/kg) relative to the lignite coals (Table 2). The feed fuel blend composition was largely a result of the lignite coal and petroleum coke in the blend. Thus, the feed fuel blend burned at PS2 showed remarkable concentrations of Cr (78 mg/kg), Zn (103 mg/kg), Ni (65 mg/kg), and Pb (40 mg/kg).

Distinctions identified in the chemical composition of the PS3 lignite coal and contrasted with the PS1 and PS2 lignites revealed lower concentrations of all the HTEs in the PS3

https://doi.org/10.1021/acsomega.1c07326
ACS Omega 2022, 7, 14697−14711

lignite except for Mo. These HTEs also marked a difference, in terms of concentration, over the rest when comparing the chemical composition of the lignite coals with their average contents in the coal of China[20] and worldwide.[21] The average concentrations of As, Cr, Ni, Zn, and Pb in lignite coals were remarkably higher than those in both the Chinese and worldwide coal concentration ranges.

Quartz (SiO_2), muscovite [$KAl_2(AlSi_3O_{10})(OH_2)$], and kaolinite ($Al_2Si_2O_5(OH)_4$) with traces of calcite ($CaCO_3$), pyrite (Fe_2S), and anatase (TiO_2) were the main crystalline phases of the PS1 and PS3 lignite coals. These same phases were also identified in the PS2 feed coal along with gypsum ($CaSO_4{\cdot}2H_2O$), clinochlore [$(Mg; Fe^{2+})_5Al(Si_3Al)O_{10}(OH)_8$], and illite [$(K,H_3O)(Al, Mg, Fe)_2(Si, Al)_4O_{10}$].

3.2. Characterization of CCPs. *3.2.1. FA, FBC Ashes, BS, and BAs.* PS1 FA consisted of an aluminosilicate glassy matrix with a high content of quartz and minor proportions of muscovite. The scanning electron microscopy (SEM)−EDX photomicrographs displayed in Figure 1a show that the PS1 FA contains fine, predominantly spherical particles, both solid and hollow, and mostly glassy (amorphous). Large amounts of spherical FA particles, as shown in Figure 1a photomicrographs, suggest they are possibly solidified from a viscous fluid state.[25] On the other hand, the hollow spherical shape is due to the expulsion of gaseous materials from the particle interior, owing to an increase in internal pressure or a decrease in external pressure. The main elements in the PS1 FA surface include Si, Al, Ca, K, Mo, Ti, O, and Fe. Fe-crystalline species, such as hematite (Fe_2O_3) and magnetite (Fe_2O_4), occur within the glass particles (i.e., segregated from the melt during the combustion process). Similarly, PS1 BS was characterized by the predominance of an aluminosilicate glass matrix with high contents of quartz and traces of calcite. Notably, PS1 BS demonstrated similar yet relatively higher concentrations of minor and trace elements such as Cr, Mn, Ni, As, and Se FA as featured in Tables 3 and 4.

The PS2 ash consisted of an aluminosilicate glassy matrix with quartz and minor proportions of muscovite, anhydrite ($CaSO_4$), and hematite. The SEM−EDX photomicrographs in Figure 1b show that particles are highly diversified concerning sizes and shapes, evidencing some porous structures with several smaller particles covering their shells. Pseudospheres, spherical particles composed of various layers or grains, are also noted. In addition, SEM−EDX indicates that the PS2 ash is composed mainly of irregularly shaped particles, in contrast to the primarily spherical PS1 products. This difference is due to the lower temperature of FBC technology (700−900 °C) compared to that of PCC (1300−1700 °C), which was insufficient to melt irregularly shaped FA particles into spheres. However, fundamental operating conditions such as the fuel type[22] and/or the nature and quantity of used adsorbent material can also define FA particle shape and its physical properties. The main elements in the PS2 ash surface include Si, Al, Ca, O, K, Mo, Cu, and Zn. The PS2 BA was also characterized by the predominance of an aluminosilicate glass matrix with quartz and minor proportions of muscovite and anhydrite along with calcite and anatase (TiO_2). The PS2 ash is, conversely, enriched (FBC ash/BA > 1.3) in S, Sr, B, Zn, Ga, Ge, Se, As, Mo, Sn, Sb, Pb, and especially Hg, as shown in Tables 3 and 4.

The PS3 ash consisted of an aluminosilicate glassy matrix with quartz and minor proportions of muscovite, anhydrite, calcite, hematite, and lime (CaO). The PS3 ash is composed

Table 3. Average Concentration of Major, Minor, and Trace Elements in PS1 FA, PS2 Ash, and PS3 Ash[a]

%	PS1-FA	PS2-ash	PS3-ash
Al_2O_3	27	27	26
CaO	2.5	2.9	10
Fe_2O_3	5.6	4.9	4.7
K_2O	2.7	2.7	2.6
MgO	1.2	1.3	1.3
Na_2O	0.5	0.7	0.7
P_2O_5	0.2	0.2	0.2
SO_3	0.4	2.4	8.1
mg/kg	PS1-FA	PS2-ash	PS3-ash
Cl	692	807	709
Hg	0.3	0.7	0.7
Li	107	116	134
Be	3.2	3.8	5.7
B	632	85	77
Sc	22	28	26
Ti	5375	4355	4409
V	192	562	577
Cr	106	146	144
Mn	161	137	125
Co	15	20	18
Ni	68	149	226
Cu	81	85	86
Zn	120	138	129
Ga	39	42	33
Ge	7.9	17	16
As	14.8	43	35
Se	3.8	5.7	6.6
Rb	280	224	208
Sr	160	182	193
Y	28	43	43
Zr	132	141	146
Nb	14	12	14
Mo	2.9	8.8	8.2
Sn	4.1	5.2	4.4
Sb	12	72	82
Cs	39	32	29
Ba	620	1078	1035
La	64	48	48
Ce	98	112	116
Pr	11	11	11
Nd	48	51	35
Sm	10	10	8.9
Eu	2.1	2.1	2.2
Gd	7.6	8.1	7.3
Tb	1.2	1.0	1.3
Dy	6.8	7.8	7.0
Ho	1.6	1.3	1.5
Er	4.8	4.1	3.6
Yb	4.3	5.7	3.3
Lu	<dl	0.8	<dl
Hf	5.5	4.6	4.2
Ta	1.1	<dl	<dl
W	4.0	27	19
Tl	1.5	1.4	1.5
Pb	36	46	41
Th	41	18	22
U	8.2	29	34

[a]FA: fly ash.

https://doi.org/10.1021/acsomega.1c07326
ACS Omega 2022, 7, 14697−14711

Table 4. Average Concentration of Major, Minor, and Trace Elements in PS1 BS, PS2 BA, and PS3 BA[a]

%	PS1 BS	PS2 BA	PS3 BA
Al	19	11	22
Ca	2.2	2.5	15
Fe	4.2	3.3	6.5
K	2.9	1.7	3.3
Mg	0.9	0.6	1.1
Na	0.5	0.3	0.7
P	0.1	0.05	0.1
S	1.0	0.2	5.2
mg/kg	PS1 BS	PS2 BA	PS3 BA
Cl	1021	677	830
Hg	0.02	0.004	0.02
Li	139	92	208
Be	4.1	2.3	5.8
B	610	621	89
Sc	33	19	39
Ti	7220	4016	8270
V	300	198	484
Cr	148	184	223
Mn	180	221	361
Co	19	8.8	23
Ni	86	61	141
Cu	79	47.0	93
Zn	181	84.0	259
Ga	46	18.0	54
Ge	11	3.9	14
As	17	11.6	69
Se	7.7	4.3	8.7
Rb	321	206	352
Sr	211	126	255
Y	36	52	58
Zr	179	261	233
Nb	21	22	31
Mo	9.9	2.1	10
Sn	8.3	2.0	8.9
Sb	32	12	55
Cs	60	30	51
Ba	776	600	1055
La	75	48	98
Ce	160	121	167
Pr	17	10	19
Nd	69	52	68
Sm	11	11	13
Eu	2.2	2.0	3.3
Gd	8.0	7.3	11
Tb	1.0	1.1	1.3
Dy	8.1	7.2	12
Er	4.3	5.7	5.7
Tm	1.0	1.1	1.1
Yb	5.4	6.1	5.6
Lu	0.9	0.0	1.1
Hf	6.8	5.3	7.5
Ta	1.4	1.1	1.2
W	7.6	4.4	15
Tl	2.8	2.2	2.2
Pb	52	25	79
Th	32	25	38
U	13	9.7	23

[a]BS: boiler slag and BA: bottom ash.

largely of irregularly peaky-shaped particles (Figure 2) consisting of different inorganic phases and possibly a certain quantity of unburned organic materials. These irregular grains and agglomerations usually correspond to calcite, which was identified by XRD. The SEM−EDX photomicrographs in Figure 1c emphasize the peaks of the PS3 ash particles relative to the PS2, which could be ascribed to the different types of fuel burned at PS2 (lignite + petcoke) and PS3 (lignite coal). Both operated under similar FBC conditions (i.e., combustion temperature, Ca-bed material, particulate control device, etc.).

The PS3 BA was distinguished by an aluminosilicate glass matrix containing high contents of quartz and minor proportions of muscovite, anhydrite, and calcite. The PS3 BA demonstrated substantially higher concentrations of minor and trace elements such as Ti, Cr, Mn, Rb, Pb, As, and Se than the PS3 FBC FA as displayed in Tables 3 and 4.

Crystalline phases in the FA/FBC ash and their morphological properties chiefly rely on the type of combustion technology utilized. FA generated during PCC was predominately spherical and glassy, while the ashes from FBC constituted irregularly or angularly shaped particles with quartz, calcite, anhydrite, lime, and/or portlandite [$Ca(OH)_2$] as the main crystalline phases because of the Ca-sorbent material used in in-bed desulfurization during FBC.

Distinctions identified in the chemical composition of the PS2 and PS3 ash compared against the PS1 FA revealed that major elements Ca and S were substantially enriched in both the PS2 and PS3 ash (2.9−10% as CaO and 2.4−8.1% as SO_3) relative to the FA (2.5% CaO and 0.4% SO_3) due to the direct reaction of the limestone used to form the combustion bed with SO_x. Besides Ca and S, the PS2 and PS3 ash were highly enriched in V by up to a factor of 2.5−2.9 and in Ni (2.5−3.1), Cr (1.3), Zn (1.2), As (1.9−2.6), Se (1.5−1.7), Mo (2.9), Sb (4.0−5.1), Pb (1.2), U (2.7−3.1), and especially in Hg with respect to the FA at PS1 (Table 2). Trace element concentrations, found to be higher in the FBC ash at PS2 and PS3 with respect to FA at PS1, can be explained by the fundamental operating conditions of the combustion technology. For example, the in-bed desulfurization during FBC used a Ca-sorbent material. At the PS2 and PS3 boilers, that might contribute an appreciable amount to the trace element content due to impurities, for example, rhodochrosite ($MnCO_3$), cerussite ($PbCO_3$), smithsonite ($ZnCO_3$), and sulfide minerals. However, the particulate control device, along with the characteristics of the ash collected in it, can also play a significant role in this observation. At PS2 and PS3, the particulate control is based on BFs (baghouses), which have a similar overall particulate removal efficiency to ESP (>99%) but thrive at controlling fine PM.[26] It is in the finer particles where trace elements tend to receive enrichment due to their larger specific surface area, which allows greater condensation or surface adsorption of volatile elements. Indeed, the PS2 (7.6031 ± 0.0321 m^2/g) and PS3 (6.0283 ± 0.0456 m^2/g) ashes have higher specific surface areas than the PS1 FA (2.0485 ± 0.0335 m^2/g), which confirms the theory of higher enrichment of the FBC ash relative to PCC FA. The BET surface area report of the PS1 FA and PS2 and PS3 is provided in the Supporting Information (Table S7).

3.3. Chemical Speciation of Hazardous Elements.

3.3.1. Chemical Speciation of Hazardous Elements in Fuels.

The chemical speciation of HTEs in Table 5 shows that the mass balance rate of all the HTEs in the lignite coals and feed

https://doi.org/10.1021/acsomega.1c07326
ACS Omega 2022, 7, 14697−14711

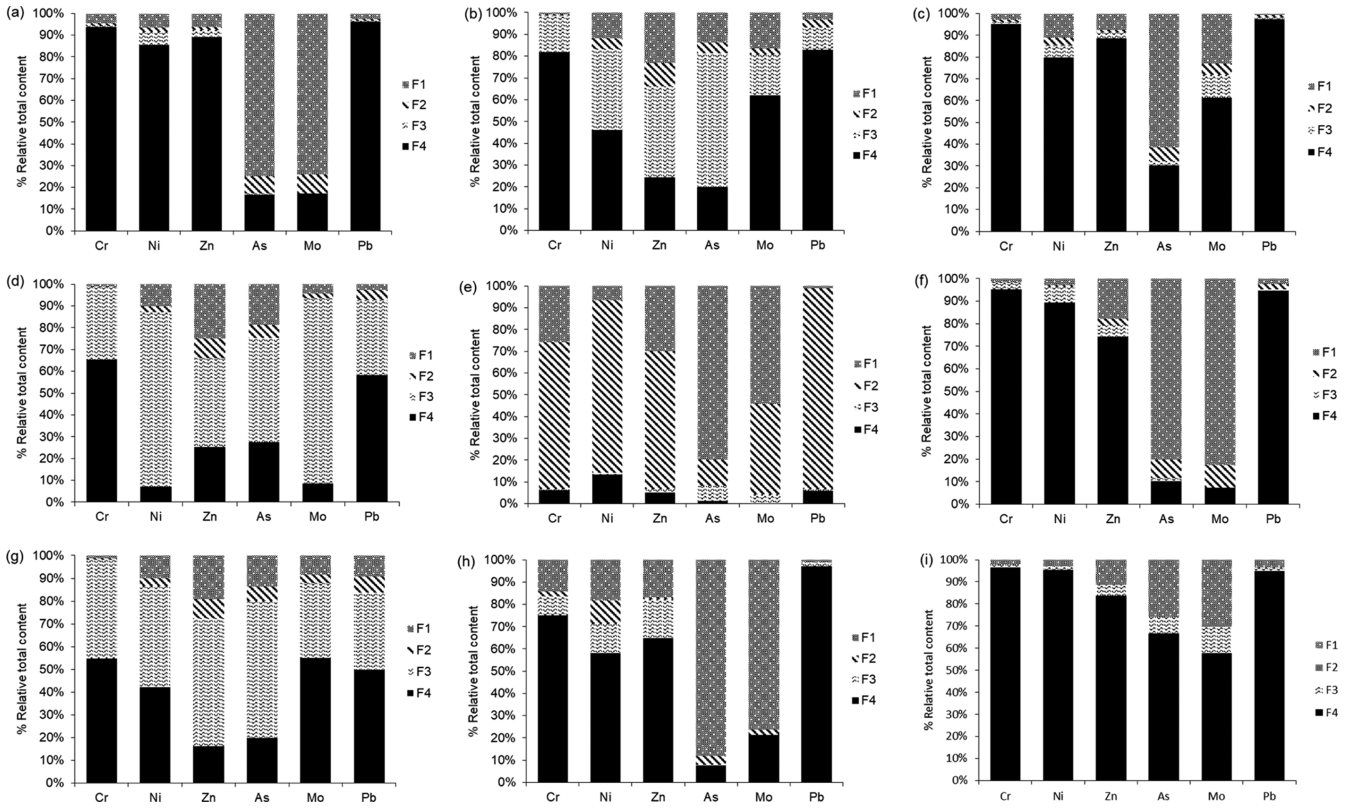

Figure 2. Chemical speciation ratio of HTEs in the (a) PS1 LC, (b) PS1 FA, and (c) PS1 BS; (d) PS2 FB, (e) PS2 ash, and (f) PS2 BA; and (g) PS3 LC, (h) PS3 ash, and (i) PS3 BA based on the modified BCR sequential extraction method (F1: water/acid-soluble and exchangeable fractions; F2: reducible fraction; F3: oxidizable fraction; and F4: residual fraction).

fuel blend ranged from 103 to 110%, demonstrating the reliability of the chemical speciation analysis and data.

The lignites and feed fuel blend had a relatively high abundance of As (73−80%) due to the mobile fraction ($\sum$F1 + F2 + F3), in particular, with the organic matter and sulfides (F3) as shown in Figure 2. The chemical speciation of As in these lignite coals and feed fuel blends matches the most common occurrence of As in coals as arsenopyrite (FeAsS).[27−32] However, some coals contain As in other forms such as organic,[33] clay, and/or phosphate associations.[34] Even rare and unusual modes of occurrence of As such as that of getchellite ($AsSbS_3$)[35] have also been noted.

The selective leaching results for Mo in the lignite coals and feed fuel blend were consistent with multiple modes of occurrence. While the relative abundance of Mo (92%) in the mobile fraction was remarkably high in the PS2 feed fuel blend, mainly due to its major association with both organic matter and sulfides, 62% and 55% of Mo in the non-mobile fraction were strongly bound to the amorphous and crystalline structures in the PS1 and PS3 F4 lignite phases, respectively. Minor abundances of Mo (19 and 33% in PS1 and PS3) were owed to the presence of organic matter and sulfides (Figure 2). Nevertheless, a recent study[36] indicated that Mo does not have strong chalcophile tendencies (i.e., bond with S as a highly insoluble sulfide) in coal because of the large spectrum of occurrences within the coal rank. They found that approximately 30% of Mo in bituminous coals remained unleached, as did about 45% in low-rank coals, which was attributed likely due to the association of Mo with organics and/or shielded mineral grains.

The selective leaching results indicate that most of the Pb (83%) in the PS1 coal is tied to the non-mobile fraction strongly bound to structures of amorphous and crystalline phases (F4) (Figure 2). Concerning the PS2 feed fuel blend and PS3 lignite, the chemical speciation of Pb in comparison showed a twofold association with both the non-mobile fraction (50−58%) and organic matter and sulfides (34−35%). Based on previous studies,[29,30] Pb is inorganically bound in coals, where substantial amounts in the Appalachian Basin coals occur as PbSe (claustalite). However, in most other coals, authors[29,30] reported that the dominant brand of Pb was galena (PbS), with some occurring in sulfates, carbonates, phosphates, and silicates, especially in sulfide-poor coals. It can, therefore, be concluded that Pb, as with Mo, shows multiple modes of occurrence in coals with no clear pattern and/or association.

Chromium largely occurred in the non-mobile fraction (residual) of the PS1 (82%) and PS3 (55%) lignite coals and the PS2 feed fuel blend (65%), as displayed in Figure 2. However, the rate of oxidizable Cr in the fuels was in the range of 17−43%, which indicates that a substantial part of the Cr was related to organic matter and sulfides. This chemical speciation of Cr would be in line with the first observations made by Swaine,[34] who reported a reasonably organic association of Cr in low-rank coals. Finkelman[29,30] and Huggins et al.[37] concluded, however, that Cr is likely to be associated with clays where some Cr accompanies spinel group minerals such as chromite ($FeCr_2O_4$).

Although no insights are available about the specific mode of occurrence of Zn in lignite coals, it has been reported that the bulk of Zn in mostly bituminous coal is found in pyrite and other sulfides [e.g., sphalerite (ZnS)]. Alternatively, some Zn

https://doi.org/10.1021/acsomega.1c07326
ACS Omega 2022, 7, 14697−14711

Table 5. Chemical Speciation Concentration of HTEs in the PS1 LC, PS1 FA, and PS1 BS; PS2 FB, PS2 Ash, and PS2 BA; and PS3 LC, PS3 Ash, and PS3 (F1: Water/Acid-Soluble and Exchangeable Fractions; F2: Reducible Fraction; F3: Oxidizable Fraction; and F4: Residual Fraction)

	Cr	Ni	Zn	As	Mo	Pb
			PS1			
			lignite coal			
F1	0.7	4.5	16	1.8	0.4	1.2
F2	16	14	29	8.0	0.5	3.5
F3	0.5	1.8	7.2	0.6	0.1	1.3
∑F + residue	92	38	68	13	2.4	35
pseudo total	89	45	95	12	2.8	31
MB	103	85	72	111	85	113
			PS1 FA			
F1	5.0	3.6	7.6	15	2.0	0.9
F2	0.8	3.3	3.9	0.1	<0.01	0.1
F3	1.2	1.0	1.5	1.5	0.2	0.3
∑F + residue	112	55	120	20	2.7	34
pseudo total	121	65	119	18	3.2	37
MB	92	84	101	109	83	92
			PS1 BS			
F1	5.3	9.0	35	6.7	0.4	7.2
F2	1.4	13	9.5	0.7	0.2	0.3
F3	1.9	1.6	5.5	0.9	0.1	0.4
∑F + residue	133	78	171	21	11	63
pseudo total	164	74	167	19	11	51
MB	81	105	102	108	107	124
			PS2			
			PS2 FB			
F1	0.8	6.0	27	2.2	0.2	0.8
F2	0.4	1.6	9.7	0.7	0.1	1.2
F3	30	47	43	5.7	3.9	9.3
∑F + residue	90	59	107	12	4.6	27
pseudo total	82	60	102	12	4.2	30
MB	110	98	105	99	110	88
			PS2 ash			
F1	38	10	46	36	5.8	0.5
F2	1.0	1.4	2.2	3.1	0.4	0.4
F3	9.2	21	8.1	0.6	0.0	3.2
			PS2 ash			
∑F + residue	148	154	154	45	11	53
pseudo total	156	165	145	48	10	45
MB	95	93	106	93	112	117
			PS2 BA			
F1	45	27	26	10	1.8	3.5
F2	0.9	0.4	4.9	0.8	0.3	3.5
F3	13	4.6	5.2	0.1	<0.01	0.1
∑F + residue	98	60	55	11	2.3	16
pseudo total	110	57	66	9.2	2.3	19
MB	89	104	83	125	101	82
			PS3			
			PS3 LC			
F1	0.6	3.1	11	1.1	0.1	1.2
F2	0.3	1.1	4.6	0.5	0.0	0.9
F3	21	14	31	4.9	0.4	4.3
∑F + residue	27	31	56	8.2	1.3	13
pseudo total	48	37	47	5.9	1.3	16
MB	105	85	118	139	100	81
			PS3 ash			
F1	17	33	22	25	7.9	0.5
F2	2.5	19	1.1	1.2	0.2	0.1
F3	9.8	24	23	0.1	<0.01	0.6
∑F + residue	116	183	130	29	10	43
pseudo total	140	204	134	35	9.1	42
MB	83	90	97	83	115	101
			PS3 BA			
F1	12	19	77	38	7.7	2.6
F2	0.04	0.1	0.4	<0.01	0.04	<0.01
F3	9.7	22	52	5.0	1.1	1.1
∑F + residue	192	136	235	58	9.1	73
pseudo total	221	138	247	58	9.4	76
MB	87	98	95	100	97	96

in low-rank coals may be organically bound and express a minimum abundance (~25%) than those normally associated with silicates,[29,30] which would be consistent with the chemical speciation of Zn in these lignites (Figure 2).

Nickel appears in coal so broadly and diversely that it has been postulated to be organically associated, inorganically bound by association with sulfides[29,30] and/or occur in clays. In this study, Ni showed a twofold association in the PS1 lignite with organic matter and sulfides (37%), and the non-mobile fraction was strongly bound to structures of amorphous and crystalline phases (46%). In the PS2 feed fuel blend, 80% of Ni was bound to organic matter and sulfides, while a minor abundance (10%) occurred in the most bioavailable fraction (i.e., easily soluble, F1). Nickel in the PS3 lignite also showed a twofold association with organic matter and sulfides (44%) and the non-mobile fraction was strongly bound to structures of amorphous and crystalline phases (42%) (Figure 2). Despite a reasonable amount of uncertainty about how Ni manifests in coal, the results of our study to some extent coincide with the speciation of Ni in lignites from the Kosovo basin, Yugoslavia, where it was found[38] that approximately 10% of the Ni was organically associated and that most of the inorganic Ni occurred in spinels.

The selective leaching results indicate that most of the V in the PS1 (62%) and PS3 (58%) coals were associated with organic matter and sulfides. A minor proportion (33% PS1 and 23% PS3) appeared in the non-mobile fraction, strongly bound to structures of amorphous and crystalline phases (Figure 2). The chemical speciation of V changes in relation to the PS2 feed fuel blend, where V is mostly associated (94%) with the organic matter due to the petroleum coke in the blend. These results suggest that both lignites and lignite-petcoke blends had a relatively high abundance of V (77−99%) associated with the mobile fraction (∑F1 + F2+ F3), which is consistent with what Finkelman,[29,30] Palmer and Filby,[39] and Li et al.[26] reported. These authors concluded that V is generally associated with organic matter and, to a lesser extent, with clays and other minerals.

The association of inorganic trace elements in coal with the organic fractions has been extensively studied, but there exist more observations to reconcile. Coals of varying ranks may show different elemental associations, as do coals of the same rank from differing geographic areas.

3.3.2. Chemical Speciation of Hazardous Elements in FAs, BS, and BA. The chemical speciation of HTEs in Table 4 shows that the mass balance rate of all the HTEs in the FA was

https://doi.org/10.1021/acsomega.1c07326
ACS Omega 2022, 7, 14697−14711

in the range of 93−117% but 81−124% in the BS/BA, which shows the reliability of the chemical speciation analysis and data.

The relative content of mobile HTEs (F1+ F2 + F3) within the PS1 FA showed the following order of abundance: As (85%) > Mo (83%) > Ni (14%) > Zn (11%) > Cr (6.2%) > Pb (3.8%), where As and Mo were almost entirely (74−77%) within the easily soluble fraction (F1).This would entail a threat to the environment, as shown in Figure 2b. The non-mobile fraction consisted mostly of Cr (94%) > Zn (89%) > Ni (84%).

In the BS from PS1, the order of relative abundance within the mobile fraction was, as also shown in Figure 3c, As (29%) > Ni (16%) > Zn (14%) > Mo (6.6%) > Cr (6.5%), and Pb (1.6%), which indicates that most of the HTEs were connected to the non-mobile fraction.

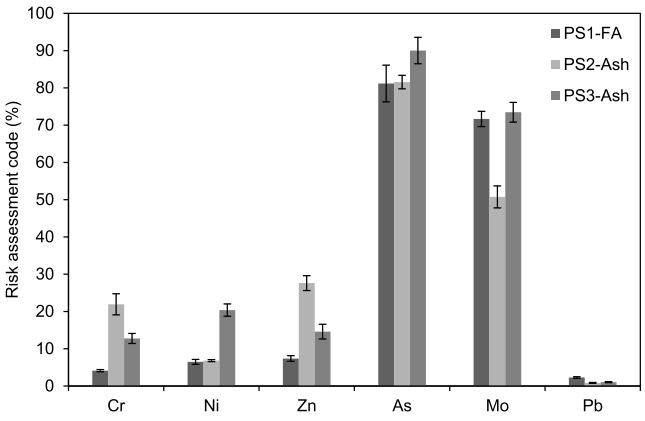

Figure 3. RAC of HTEs in the PS1 FA, PS2 ash, and PS3 ash.

In the PS2 ash, the order of relative abundance of HTEs within the mobile fraction was, as also presented in Figure 2e, Mo (100%) > As (99%) > Zn (95%) > Cr and Pb (94%) > Ni (87%). Molybdenum was associated with the easily soluble fraction (54%), and bound to Fe and/or Mn oxyhydroxides (42%), which could be released depending on the redox conditions in the environment. The addition of petcoke to the feed fuel changed the leachable patterns of most HTEs compared to PS1 and PS3. Arsenic (80%) and V (53%) were largely within the most bioavailable fraction (easily soluble, F1). Lead (92%), Ni (79%), Cr (67%), and Zn (64%) were associated with the reducible fraction, bound to Fe and/or Mn oxyhydroxides, with minor abundance (1−6.2%) bound to structures of amorphous and crystalline phases.

The PS2 BA mobile fraction showed substantial amounts of Mo (93%) and As (90%). Of them, 80% of Mo and 83% of As were associated with the easily soluble fraction, while Pb (95%), Cr (95%), Ni (89%), and Zn (74%) were bound to the non-mobile fraction. Figure 2f presents these developments.

As shown in Figure 2h, the relative content of mobile HTEs within the PS3 ash expressed an abundance of As (92%) and Mo (79%), followed by Ni (42%), Zn (35%), Cr (25%), and (Pb), where As (88%) and Mo (76%) were largely within the easily soluble fraction. Lead (97%), Cr (75%), Zn (65%), and Ni (58%) were bound to structures of amorphous and crystalline phases with minor abundance (8.4−17%) related to organic matter and sulfides.

The PS3 BA showed a distribution of metal mobility similar, to a certain extent, to that shown by the BS produced during PCC, where As (67%), Mo (58%), and the rest of the HTEs remained bound to the non-mobile fraction (Figure 2i).

3.4. Fractionation and Dynamics of HTEs Across Combustion. *3.4.1. Fractionation of Elements during Combustion.* The fractionation of elements during the combustion process (Figure S1) is summarized as follows:

(i) Elements enriched in FA/FBC ash ($EF_{FA/FBC\ ash}/EF_{BS/BA}$ concentration ratio ≥ 1.2) included, in increasing enrichment order, Cr, Zn, Pb, Ni, Mo, and As at PS2; Mo and Ni at PS3; and slight amounts of As and Ni at PS1 (Figure 3). The enrichment of these elements originates from their volatilization during combustion, followed by condensation onto FA/ash surfaces in the flue gas during cooling (i.e., when the temperature drops to ∼120 °C along the boiler-ducts-air-preheater-ESPs or BF line).

(ii) Elements enriched in BS or BA ($EF_{FA/FBC\ ash}/EF_{BS/BA}$ concentration ratio < 0.9) included Mo in the BS from PS1.

(iii) Elements with no clear segregation between FA/FBC ash and BS/BA ($EF_{FA/FBC\ ash}/EF_{BS/BA}$ concentration ratios between 0.9 and 1.1) included Pb, Cr, and Zn at PS1 and As, Pb, Cr, and Zn at PS3.

Our initial evaluation of the singular segregation of Mo in the BS from the PS1, although discussed in detail in the next section, led us to suggest that it could be due to the relatively high content of Fe (4.9% as Fe_2O_3) in the BS along with the combustion operating conditions. Fe species such as hematite are efficient sinks for metals to such an extent that enrichments of Mo in sediments have been attributed to adsorption into Fe and Mn oxides.[40−43] Córdoba et al.[44] evaluated chemical stabilization methods of coal-petcoke FA in order to reduce the mobility of Mo and Ni by using both goethite [α-FeO(OH)] and a BS generated at a coal-fired power station. Although the results of this study failed to support Fe oxides as an efficient option to reduce the potential leaching of Mo in FA leachates, we concluded that the enrichment of Mo in the BS possibly happened once the molten slag collected from the base of the boiler came into contact with the quenching water, leading to its fracturation and crystallization. At this instant, Mo can be adsorbed by Fe oxides. This could also serve as the mechanism by which most trace elements are enriched in the BS relative to PCC FA. PS1 BS demonstrated similar and even relatively higher concentrations of minor and trace elements such as Cr, Mn, Ni, As, and Se in FA.

3.4.2. Behavior of HTEs across Combustion. The differences in operating conditions and technologies among the three power stations resulted in significant divergences in the chemical speciation of the FA and FBC ashes and in the BS and BA. To clarify, in-bed desulfurization occurred in the boiler at PS2 and PS3, the fuel type (e.g., petcoke) was burned along with lignite at PS2, the combustion temperature varied (i.e., 700−900 °C FBC vs 1300−1700 °C PCC), and other such variances played a factor, such as a Ca-bed material, particulate control device, and so forth.

Four-step sequential extraction evaluated the chemical speciation of HTEs, the lignites, and the feed fuel blend, and in the CCP, so that the two dominant reaction pathways for these key HTEs across the coal combustion process could be identified.

The *gas-to-gas reaction* consists of the hydration of gaseous HTEs upon reaction with the flue gas moisture and displays

https://doi.org/10.1021/acsomega.1c07326
ACS Omega 2022, 7, 14697−14711

enrichment in fine particles of FA/FBC ash via condensation when the flue gas temperature drops.

The *gas-to-particle* reaction is based on the chemisorption of gaseous HTEs onto FA/FBC ash particles, where two mechanisms would be feasible. On the one hand, gaseous HTEs (e.g., either oxides, chlorides, and/or sulfates including hydrated forms) can react mainly with Ca- and Fe-based cations and other alkaline elemental oxides sites available on FA/FBC ash surfaces to form stable compounds (surface-bound pollutants of ultrafine FA particles). On the other hand, gaseous HTEs interact with FA/FBC ash constituents (e.g., SiO_2 and Al_2O_3) and incorporate themselves into the structures of amorphous and crystalline phases of the FA/FBC ash.

In the lignite coals and feed fuel blend, As is associated with organic matter and sulfides. It mostly occurs as arsenopyrite. During combustion, whether PCC or FBC, As is volatilized, typically as $As_2O_{3(g)}$; however, $AsCl_{3(g)}$ would be the main speciation in high chlorine−coal combustion[42] and may go through several reaction pathways in the post-combustion atmosphere. Gaseous $As_2O_{3(g)}$ may remain in the gaseous phase and/or react with flue gas moisture to form $H_3AsO_{4(g)}$, which would condense upon entering the FGD. Alternatively, gaseous As_2O_3 may adhere to FA/FBC ash particles when contact is adjacent to an active cation surface site in a process called attractive bonding. Calcium and Fe serve as the main cation sites available on FA/FBC ash surfaces where $As_2O_{3(g)}$ could be chemisorbed onto the FA/FBC ash surface. This primarily manifests as them reacting with CaO and/or Fe_2O_3 to form calcium arsenate ($Ca_3(AsO_4)_2$) and/or iron arsenate ($FeAsO_4$), respectively, which would explain how As acted in the PS1 FA and PS2 and PS3 ashes within the most bioavailable fraction (easily soluble, F1).

In the PS2 BA, As is entirely associated with the easily soluble fraction, meaning that interactions with Ca- and Fe-based cations would lead to the retention of As onto the BA. A different reaction pathway would be followed by As in the PS1 BS and PS3 BA, where it is postulated that some As would be trapped in the liquid matrix minerals due to short residence time in the combustion zone, explaining their association with their non-mobile fraction.

Molybdenum is mostly associated with organic matter, sulfides, and other petcoke species in the PS2 feed fuel blend, but it also shows a major association with the non-mobile fraction strongly bound to structures of amorphous and crystalline phases in the PS1 and PS3 lignites. During combustion, Mo is released mostly as molybdenum trioxide (MoO_3) and/or molybdic acid (H_2MoO_4) and may follow a similar reaction pathway to that of As. Gaseous $MoO_{3\ (g)}$ may remain so and/or react with flue gas moisture to form $H_2MoO_{4\ (g)}$, which would condense upon entering the FGD. Alternatively, $H_2MoO_{4\ (g)}$ could also be chemisorbed onto the FA/FBC ash surface via reaction either with CaO, MgO, and/or Na_2O to form stable forms of calcium molybdate ($CaMoO_4$), magnesium molybdate ($MgMoO_4$), and sodium molybdate (Na_2MoO_4). Thus, that could be how it associates with the most bioavailable fraction (F1) in the PS1 FA and PS2 and PS3 ashes. The consistency of our postulated reaction pathways for Mo relies on the fact that Ca-, Mg-, and Na-based sorbents have shown a strong affinity for Mo at low to medium post-combustion temperatures.[45] This interaction would, to a certain extent, represent the combustion conditions under which Mo is released as $MoO_{3(g)}$ and/or $H_2MoO_{4(g)}$ and reacts with Ca-, Mg-, and Na-based cations sites available on FA and FBC ash surfaces. Moreover, as we mentioned above, Fe species such as hematite can also be an efficient sink for Mo via adsorption into Fe oxides,[40,41] which would be in line with the speciation of Mo in the PS2 ash, where 42% of Mo is bound to either Fe and/or Mn oxyhydroxides.

In the PS2 BA, Mo is entirely associated with the easily soluble fraction, meaning that interactions with Ca-, Mg-, Na-, and Fe-based cations would also occur and lead to the retention mechanism based on an association of Mo with the liquid matrix minerals (silicates) of the BS and BA. This would explain the major association of Mo with the non-mobile fraction in PS1 BS and PS3 BA.

Lead shows multiple modes of occurrence in the studied fuels, but its association with the non-mobile fraction predominates over the rest. During combustion, Pb is released and transferred to the gas phase. Temperatures reach upward to 850 °C, allowing it to exist as $PbO_{(g)}$, but it can change over into $PbO_{(s)}$ when the flue gas cools down to 730 °C. Any lower, and it would instead occur as $PbSO_4$.[46] Depending on the dew points of the gaseous Pb species, Pb would condense (e.g., PbO or $PbSO_4$) onto the FA/FBC ash when the flue gas cools down along the boiler-ducts-air-preheater-ESPs or be incorporated into the aluminosilicate matrix of the FA/FBC ash by reaction with ash constituents. The latter reaction pathway would tally with how Pb is associated with the structures of the amorphous and crystalline phases of the PS1 FA and PS3 ash. The reaction pathway Pb follows in the PS2 ash would instead be based on adsorption of Pb on Fe oxides (e.g., goethite or ferrihydrite) due to the abundant binding sites of Fe, where Pb(II) would form inner-sphere complexes on goethite or ferrihydrite surfaces[47] onto the FA. The reaction pathway that allows Pb to be incorporated into Fe oxides has been widely studied and could explain the speciation of Pb in the PS2 ash, where 92% of Pb is bound to either Fe and/or Mn oxyhydroxides.

Chromium boasted a clear association with the non-mobile fraction in all the studied fuels. However, the significant rate of oxidizable Cr in the fuels indicates that a substantial part of the Cr was related to organic matter and sulfides. During combustion, Cr is mostly released in the form of $CrO_{3(g)}$,[48] either as a gas or reacting with flue gas moisture in the presence of S (either gaseous H_2SO_3 or H_2SO_4) to produce $CrO_2(OH)_2$ (where other derived gaseous Cr species could also be formed) and condensing upon entering the FGD. Otherwise, gaseous $Cr_2O_{3(g)}$ and $CrO_2(OH)_2$ would adhere to FA/ash particles via reaction with CaO or other alkaline elemental oxides to form $CaCrO_4$ or $(Mg, K, Na, Fe)CrO_{4(s)}$[49] and/or with Fe oxyhydroxides (e.g., goethite or ferrihydrite) on the ash surface where adsorption takes place. These reaction pathways would explain the speciation of Cr in the PS2 ash, where 67% of Cr is bound to Fe and/or Mn oxyhydroxides and 26% to the bioavailable fraction. However, the interaction of Cr with ash constituents (e.g., SiO_2 and Al_2O_3) would be the path taken by Cr in the PS1 FA and PS3 ash, where it ultimately incorporates into their amorphous and crystalline matrices.

Vanadium showed a twofold association mostly with organic matter and sulfides, and the non-mobile fraction was strongly bound to the structures of amorphous and crystalline phases in the studied fuels. During combustion, V becomes gaseous (e.g., $V_2O_{5(g)}$). The reaction pathway followed by V in the PS1 FA and PS3 ash involves incorporation into the aluminosilicate

https://doi.org/10.1021/acsomega.1c07326
ACS Omega 2022, 7, 14697−14711

minerals of the ash via reaction with ash constituents as revealed by the chemical speciation. In the PS2 ash, V is chemisorbed onto the ash surface via reaction either with CaO, MgO, and/or Na_2O to form stable states such as calcium vanadate (CaV_3O_7) and/or sodium vanadate pentahydrate ($NaVO_3{\cdot}3.5H_2O$). Such is how it manifests in the most bioavailable fraction (F1) of the PS2 ash.

Zinc is found organically bound in pyrite, in other sulfides, and held some associations to silicates in the studied fuels. During combustion, Zn releases as $ZnO_{(g)}$ and could remain in a gas phase or display enrichment in fine particles of FA via condensation. However, the reaction pathway followed by Zn in the PS1 FA and PS3 ash instead hinges on its interaction with FA/ash constituents to form $2ZnO{\cdot}SiO_2$, $ZnO{\cdot}Fe_2O_3$, and $ZnO{\cdot}Al_2O_3$.[50] Through this way does it associate with the structures of amorphous and crystalline phases of the PS1 FA and PS3 ash.

Nickel showed a twofold association with organic matter and sulfides, and the non-mobile fraction was strongly bound to the structures of amorphous and crystalline phases in the studied fuels. During combustion, Ni would be released and transferred to the gas phase as oxides, chlorides, and/or sulfates as its primary forms, all of which depend on the concentration of S and Cl in the burned coal, among other factors, as combustion proceeds. Nickel would then be incorporated into the aluminosilicate minerals of the FA by reaction with ash constituents as revealed by the chemical speciation.

In the BS and PS2 and PS3 BA, Pb, Cr, Zn, and Ni were mostly associated with the structures of amorphous and crystalline phases, meaning that these HTEs would be incorporated into the aluminosilicate matrix by reaction with BS and BA constituents.

3.5. Risk Assessment. The RAC of HTEs in the lignite coals and feed fuel blend is shown in Figure 3. Lignite coals and the feed fuel blend (lignite coal + petcoke) showed no risk for Cr. Therefore, there is no significant mobility for this metal. The RAC of Pb in the lignite coals and feed fuel blend is in the range of 1−10%, while As and Zn have medium risk as per their range between 11 and 30%. The exceptions found concerning variability in risk levels are those of Mo and Ni. The PS1 lignite coal showed a medium risk for Mo and Ni, but the PS2 feed fuel blend and PS3 lignite coal showed only a low risk for both.

The RAC of HTEs in the PS1 FA and PS2 and PS3 ashes shows that there is variability in risk levels (Figure 3). Chromium and Zn in the PS1 FA and PS2 and PS3 ash samples demonstrate various risk levels, where Cr shows both low risk (PS1 FA) and medium risk (PS2 ash and PS3 ash). Nickel, conversely, shows low risk (∼6.6%) in the PS1 FA and PS2 ash and medium risk (18%) in the PS3 ash. The FA showed no risk (1.0−2.6%) for Pb; therefore, there is no significant mobility for this metal.

Molybdenum and, especially, As pose exceedingly high risks (>50%) in all the PS1 FA and PS2 and PS3 ashes, and so does V in the PS2 ash. Therefore, as potential threats to the environment, they should be given priority attention in the FA disposal process and/or in the evaluation of reuse options for this solid by-product.

3.6. Leaching Test. Distinctions identified in the leaching results compared with the waste acceptance criteria for landfills reveal that Mo in the PS1 FA (4.4 mg/kg), PS2 (2.8 mg/kg), and PS3 (2.5 mg/kg) ash leachates fall in the range of the inert material (0.5 mg/kg) established by the European Council Decision (2003/33/EC) but approach values close to those of non-hazardous waste. This supports the development of prevention measures to reduce the potential leaching of Mo, as shown in Table S6 (Supporting Information). The levels of As (0.1−0.7 mg/kg) are also in the range of the inert material (Table S6) established by the European Council Decision,[16] which also recommends that As leaching should be reduced. Although no possible comparison exists through the European waste acceptance criteria for landfills of V, it should be noted that V reaches relatively high leaching levels, especially in the PS2 (19 mg/kg) and PS3 (16 mg/kg) ash leachates.

Although the purpose of this study focuses on the selected HTEs, it should be highlighted the SO_4^{2-} leach levels from the PS1 FA, especially from the PS2 and PS3 ashes, fell within the range of inert materials. However, it had values close to those of non-hazardous waste. The F^- leach levels from the PS2 ash also reached a similar range and classification, which supports the development of prevention measures to reduce the potential leaching of F^- to meet future new standards.

The evaluation of the leaching results shows that the use of petroleum coke as a co-fuel in the PS2 causes an impact on the ash composition and, consequently, on the leaching behavior of some inorganic trace pollutants such as Mo and V. The organic affinity of Mo and V in petroleum coke favors their volatility during PCC and later condensation into the finest PS2 ash particles, which, in comparison to the PS1 FA and PS3 ash, shows enrichment in these elements.

Although no HTEs exceeded the limit for hazardous materials, As and Mo leaching yields qualify the CCPs as materials that demand prevention measures to reduce their potential leaching, which is rather a common pattern shown by these two elements in worldwide FA.[44] The high mobility and toxicity of trace elements come from the content of CaO in FA/FBC ash as it causes alkalinity in pH in their leachates, which favors the mobility of elements in their oxy-anionic form, leading to environmental leaching problems in FA. This may also reduce the reuse options of this solid residue, whether in construction engineering, the cement industry, concrete walling products, and so forth.

Some Ca additives can effectively suppress the release of anionic pollutants from FA through the formation of low-soluble Ca $(AsO_4)_3$ and $CaSeO_4$ or through the formation of ettringite ($Ca_6Al_2(SO_4)_3(OH)_{12}{\cdot}26H_2O$) and hydrocalumite ($3CaO{\cdot}Al_2O_3{\cdot}CaX2/m$).[51] The latter has also been associated with the suppression of As, B, and Se in FA leachates. In our earlier work,[52] we proved the functionality of a novel chemical stabilization method based on FA. Portlandite aggregates induce the immobilization or fixation primarily of both Mo and Ni, and of As and Se, sufficiently to reduce their concentration in the leachates to below the limits established by the European Council Decision.[18] The fixation mechanism for Mo and Ni in the FA involves portlandite aggregates ascribed to the precipitation of the $CaMoO_4$ and $NiMoO_4$ phases, respectively. The resulting FA is thus a portlandite aggregate product that could then be utilized as a substitute for concrete production, which would increase the ecological and technological benefits of this CCP.

As listed above, there are a variety of suppression mechanisms to avoid the release of anionic pollutants from FA. Despite this fact, in China still, there are irresponsible methods of disposal, including dumping ash onto land or bodies of water without proper liners or containment systems. These disposal practices are not officially reported, meaning

https://doi.org/10.1021/acsomega.1c07326
ACS Omega 2022, 7, 14697−14711

that millions of tons of ash are disposed of with no treatment, thus remaining unaccounted for.

4. CONCLUSIONS

Arsenic and Zn in an oxidizable fraction (associated with organic matter and sulfides) reach 48−60 and 41−56% of the total concentration in the studied lignite coals and feed fuel blend, respectively. The main chemical speciation of Cr and Pb is the residual form, the share of which is 55−82 and 50−83%, respectively. Molybdenum and Ni speciation are consistent with multiple modes of occurrence, existing both in a residual form in a range of 8.5−65 and 7.2−42%, respectively, and an oxidizable fraction occupying 19−85 and 37−80% of the total concentration in the lignite coals and feed fuel blend, respectively. Vanadium is mostly associated with the oxidable fraction in the feed fuel blend where it occupies 94%, which is the result of the petroleum coke contribution in the blend. In the lignite coals, the main chemical speciation of V is both the oxidable fraction, occupying 52−67% and the residual form with 33−39%.

In the PCC FA and FBC ashes, As (77−88%) and Mo (54−76%) in the water/acid-soluble and exchangeable fractions have the largest percentage compared with the other HTEs, followed by the reducible fraction. The residual form is the main chemical speciation of Cr (75−94%), Ni (58−86%), Zn (65−89%), and Pb (96−97%) in the PS1 FA and PS3 ash, while existing mainly in the reducible form (64−92%) in the PS2 ash. Vanadium has a larger percentage (52%) in the water/acid-soluble and the exchangeable fraction of the PS2 ash, which shows the effect of petroleum coke addition to the blend by increasing its mobility in the FBC ash. In the PS1 FA and PS3 ash, the residual form is the main chemical speciation of V. In the PS21 BS, all the selected HTEs are in the residual form (71−88%), while in the PS2 and PS3 ashes, the ratio of As and Mo in the mobile fraction is 33−90 and 42−93%, respectively.

The fractionation of trace pollutants during the PCC and FBC processes in the coal-fired power stations revealed group elements enriched within FA/FBC ash compared to BS/BA (EF_{FA}/EF_{BS} concentration ratio $\geq$ 1.2): these included, in increasing enrichment order, Cr, Zn, Pb, Ni, Mo, and As at the PS1, Mo and Ni at the PS3, and slightly As and Ni at the PS1. A vast majority of elements with no clear segregation between FA/FBC ash and BS/BA included Pb, Cr, and Zn at the PS1 and As, Pb, Cr, and Zn at the PS3.

Based on the RAC, Cr and Zn show low to medium risk in the PCC FA and FBC ashes, while Pb does not entail any risk at all. Molybdenum and especially As pose a worryingly high risk in all the PS1 FA and PS2 and PS3 ashes, and so does V in the PS2 ash.

Coal FAs have a diversity of developed applications, such as in engineering construction, structural fill in concrete pavements, and/or production of zeolites and geopolymers, among others, owing to their substantial production. Many of these developed applications entail coal FA−water contact, which may result in the potential release of high mobility HTEs. On the other hand, FAs not captured by ESPs, mainly in the range of nanoparticles, which are released during atmospheric emissions, may represent a high risk to the environment and public health. This is a threat to the environment, which should be given priority attention in the FA/ashes disposal process and/or in the evaluation of reuse options for this solid by-product.

The leaching results compared against the waste acceptance criteria for landfills reveal that Mo and As in the PCC and FBC ash leachates are in the range of inert materials established by the European Council Decision (2003/33/EC). Despite there being no possible comparison that can be made through the European waste acceptance criteria for landfills for V, it reaches relatively high leaching levels, especially in the PS2 and PS3 ash leachates.

The evaluation of the leaching results shows that the use of petroleum coke as co-fuel in the PS2 causes an impact on the ash composition and, therefore, on the leaching behavior of some inorganic trace pollutants such as Mo and V. The organic affinity of Mo and V in petroleum coke favors their volatility during PCC and later condensation into the finest PS2 ash particles, which, in comparison to the PS1 FA and PS3 ash, shows enrichment in these elements.

The risk of excessively contaminating FA/FBC with trace pollutants such as Mo and As is thus critical to the operation of a coal-fired power station and will directly affect the future social and economic development of coal/petroleum coke-dependent countries.

Future work will be focused on the application of our novel chemical stabilization method in the PS1 FA and PS2 and PS3 ashes, to reduce the mobility of elements such as Mo and As, and on the use of the resulting ash: the portlandite aggregate product as a substitute for concrete production.

■ ASSOCIATED CONTENT

Supporting Information

The Supporting Information is available free of charge at https://pubs.acs.org/doi/10.1021/acsomega.1c07326.

Elemental analysis (%), ash (%) and moisture (%) content, and concentration (mg/kg) of major, minor, and trace elements in the PS1 LC samples; elemental analysis (%), ash (%) and moisture (%) content, and concentration (mg/kg) of major, minor, and trace elements in the PS2 LC, PS2 PC, and PS2 FB samples; elemental analysis (%), ash (%) and moisture (%) content, and concentration (mg/kg) of major, minor, and trace elements in PS3 LC samples; elemental analysis (%), ash (%) and moisture (%) content, and concentration (mg/kg) of major, minor, and trace elements in the PS1 FA, PS2 ash, and PS3 ash samples; elemental analysis (%), ash (%) and moisture (%) content, and concentration (mg/kg) of major, minor, and trace elements in the PS1 BS, PS2 BA, and PS3 BA samples; leachable concentrations of the selected HTEs (mg/kg) from the PS1 FA and PS2 and PS3 ashes following the standard EN12457-4; BET surface area report of the PS1 FA, PS2 ash, and PS3 ash; and enrichment factors of HTEs in the PS1 FA and BA, PS2 ash and BA, and PS3 ash and BA (PDF)

■ AUTHOR INFORMATION

Corresponding Author

Patricia Córdoba − *Institute of Environmental Assessment and Water Research (IDÆA-CSIC), Spanish National Research Council, 08034 Barcelona, Spain;* orcid.org/0000-0003-0596-4354; Email: patricia.cordoba@idaea.csic.es

https://doi.org/10.1021/acsomega.1c07326
ACS Omega 2022, 7, 14697−14711

Authors

Baoqing Li − *Key Laboratory of Tectonics and Petroleum Resources, Ministry of Education, China University of Geosciences, Wuhan 430074, China*

Jing Li − *Key Laboratory of Tectonics and Petroleum Resources, Ministry of Education, China University of Geosciences, Wuhan 430074, China*

Xinguo Zhuang − *Key Laboratory of Tectonics and Petroleum Resources, Ministry of Education, China University of Geosciences, Wuhan 430074, China*

Xavier Querol − *Institute of Environmental Assessment and Water Research (IDÆA-CSIC), Spanish National Research Council, 08034 Barcelona, Spain*

Complete contact information is available at: https://pubs.acs.org/10.1021/acsomega.1c07326

Author Contributions

P.C.: conceptualization, formal analysis, methodology, writing—original draft, modeling, review and editing, and supervision. B.L.: sample collection, data curation, formal Analysis, and writing—review and editing. L.J.: writing—review and editing. X.Z.: sample collection and review and editing. X.Q.: writing—review and editing.

Notes

The authors declare no competing financial interest.

■ ACKNOWLEDGMENTS

We would like to thank the staff of the power stations for their support, help, and kind assistance during and after the sampling campaigns. The corresponding author also gratefully acknowledges the Institute of Environmental Assessment and Water Research, the Spanish National Research Council (IDÆA-CSIC), and the Excelencia Severo Ochoa Project (CEX2018-000794-S) financed by the Ministry of Science and Innovation (MINECO, Spain) and by the Generalitat de Catalunya (AGAUR 2017 SGR41).

■ REFERENCES

(1) IEA. Global Energy Review 2020; IEA: Paris, https://www.iea.org/reports/global-energy-review-2020 (accessed October 2020).

(2) BP Energy outlook. 2018, https://www.bp.com/content/dam/bp/business-sites/en/global/corporate/pdfs/energy-economics/energy-outlook/bp-energy-outlook-2018.pdf.

(3) Carbon Brief. https://www.carbonbrief.org/analysis-chinas-co2-emissions-see-first-quarterly-fall-since-post-lockdown-surge (accessed October 2021).

(4) Wang, L.; Feng, X.; Shen, L.; Jiang, S.; Gu, H. Carbon and sulfur conversion of petroleum coke in the chemical looping gasification process. *Energy* **2019**, *179*, 1205−1216.

(5) Spears, D. A.; Martinez-Tarrazona, M. R. Trace elements in combustion residues from a UK power station. *Fuel* **2004**, *83*, 2265−2270.

(6) Cui, Y. Current Situation and Development Trend of Fly Ash Utilization in China. *Institute of Technical Information for Building Materials Industry of China (ITIBMI), Coal Ash Asia Conference*, September 24, 2016.

(7) Díaz-Somoano, M.; Unterberger, S.; Hein, K. R. G. Prediction of trace element volatility during co-combustion processes. *Fuel* **2006**, *85*, 1087−1093.

(8) Córdoba, P.; Font, O.; Izquierdo, M.; Querol, X.; Leiva, C.; López-Antón, M. A.; Díaz-Somoano, M.; Martínez-Tarazona, M. R.; Ochoa-González, R.; Gómez, P. The retention capacity for trace elements by the flue gas desulphurisation system under operational conditions of a co-combustion power plant. *Fuel* **2012**, *102*, 773−778.

(9) Rodak, B. W.; Freitas, D. S.; de Oliveira Lima, G. J. E.; Reis, A. R. d.; Schulze, J.; Guilherme, L. R. G.; Guilherme, L. R. Beneficial use of Ni-rich petroleum coke ashes: product characterization and effects on soil properties and plant growth. *J. Clean. Prod.* **2018**, *198*, 785−796.

(10) Font, O.; Izquierdo, M.; Álvarez-Ayuso, E.; Moreno, N.; Diez, S.; Querol, X.; Otero, P.; Ballesteros, J. C.; Gimenez, A.; Huggins, F. E. Effect of the Addition of Petcoke on the Partitioning of Trace Elements in Pulverised Coal Combustion (PCC) Plants. *Proceedings: World of Coal Ash Conference*: Kentucky, U.S.A, 2007.

(11) European Coal Combustion Products Association (ECOBA). 2020, http://www.ecoba.com/ecobaccpspec.html.

(12) Rask, E. *Mineral Impurities in Coal Combustion, Behaviour, Problems and Remedial Measures*; Springer-Verlag: Berlin, 1985.

(13) Heidrich, C.; Feueborn, J.; Weir, A. *Coal Combustion Products: A Global Perspective*; World of Coal Ash, 2013.

(14) Heidrich, C.; Feueborn, J. *Global Operating Environment*; World of Coal Ash, 2017.

(15) Teixeira, E. R.; Mateus, R.; Camões, A. F.; Bragança, L.; Branco, F. G. Comparative environmental life-cycle analysis of concretes using biomass and coal fly ashes as partial cement replacement material. *J. Clean. Prod.* **2016**, *112*, 2221−2230.

(16) Qi, L.; Xu, J.; Liu, K. Porous sound-absorbing materials prepared from fly ash. *Environ. Sci. Pollut. Res.* **2019**, *26*, 22264.

(17) Harris, D. Ash as an Internationally Traded Commodity. *Coal Combustion Products: Characteristics, Utilization and Beneficiation*; Woodhead Publishing/Elsevier, 2017.

(18) Council Decision 2003/33/EC of 19 December 2002 establishing criteria and procedures for the acceptance of waste at landfills pursuant to Article 16 of and Annex II to Directive 1999/31/EC.

(19) Gordon, G. E.; Zoller, W. H. *Proceedings of the 1st Annual NSF Trace Contaminants Conference*; Oak Ridge National Laboratory, 1973; pp 314−325.

(20) Ure, A. M.; Quevauviller, P.; Muntau, H.; Griepink, B. Speciation of heavy metals in soils and sediments. An account of the improvement and harmonization of extraction techniques undertaken under the auspices of the BCR of the Commission of the European Communities. *Int. J. Environ. Anal. Chem.* **2006**, *51*, 135−151.

(21) Querol, X.; Alastuey, A.; Chinchón, J. S.; Fernández, J. L.; López, A. *2nd Report7220/Ed/014 European Coal and Steel Community Project*, 1993.

(22) Hao, Y.; Li, Q.; Pan, Y.; Liu, Z.; Wu, S.; Xu, Y.; et al. Heavy metals distribution characteristics of FGD gypsum samples from Shanxi province 12 coal-fired power plants and its potential environmental impacts. *Fuel* **2017**, *209*, 238−245.

(23) Dai, S.; Zhou, Y.; Ren, D.; Wang, X.; Li, D.; Zhao, L. Geochemistry and mineralogy of the Late Permian coals from the Songzo Coalfield, Chongqing, southwestern China. *Sci. China, Ser. D: Earth Sci.* **2007**, *50*, 678−688.

(24) Ketris, M. P.; Yudovich, Y. E. Estimations of Clarkes for Carbonaceous biolithes: World averages for trace element contents in black shales and coals. *Int. J. Coal Geol.* **2009**, *78*, 135−148.

(25) Kutchko, B.; Kim, A. Fly ash characterization by SEM−EDS. *Fuel* **2006**, *85*, 2537−2544.

(26) Li, F.; Zhai, J.; Fu, X.; Sheng, G. Characterization of Fly Ashes from Circulating Fluidized Bed Combustion (CFBC) Boilers Cofiring Coal and Petroleum Coke. *Energy Fuels* **2006**, *20*, 1411−1417.

(27) Clarke, L. B.; Sloss, L. *Trace Elements Emission from Coal Combustion and Gasification*; IEA- Clean Coal Centre, 1982.

(28) Crossley, H. E. Fluorine in coal. *J. Soc. Chem. Ind.* **1946**, *63*, 280−284.

(29) Finkelman, R. B. The Origin, Occurrence, and Distribution of the Inorganic Constituents in Low-Rank Coals. In *Proceedings of the Basic Coal Science Workshop*; H. H. Schobert, compiler; Grand Forks Energy Tech, Center: Grand Forks, N.D., 1981A; pp 70−90.

(30) Finkelman, R. B. Modes of Occurrence of Trace Elements in Coal. *USGS OpenFile Report*, 1981b; Vol. *81−99*, p 322.10.3133/ofr8199

(31) Stach, E.; Mackowsky, M.-T.; Teichmuller, M.; Taylor, G. H.; Chandra, D.; Teichmuller, R. *Stach's Textbook of Coal Petrology* (Translated by D. G. Murchison, G. H. Taylor and F. Zierke); Gebruder Borntraeger: Berlin, 1975, p 428.
(32) Dai, S.; Zou, J.; Jiang, Y.; Ward, C. R.; Wang, X.; Li, T.; Xue, W.; Liu, S.; Tian, H.; Sun, X.; Zhou, D. Mineralogical and geochemical compositions of the Pennsylvanian coal in the Adaohai Mine, Daqingshan Coalfield, Inner Mongolia, China: modes of occurrence and origin of diaspore, gorceixite, and ammonian illite. *Int. J. Coal Geol.* **2012b**, *94*, 250−270.
(33) Finkelman, R. B.; Belkin, H. E.; Zheng, B. Health impacts of domestic coal use in China. Proc. Natl. Acad. Sci. U. S. A. 96, 3427−3431. Francis, W., 1961. *Coal—Its Formation and Composition*; Edward Arnold Ltd: London, 1999; p 806.
(34) Swaine, D. J. *Trace Elements in Coal*; Butterworths: London, 1990; p 278.
(35) Dai, S.; Zeng, R.; Sun, Y. Enrichment of arsenic, antimony, mercury, and thallium in a Late Permian anthracite from Xingren, Guizhou, Southwest China. *Int. J. Coal Geol.* **2006**, *66*, 217−226.
(36) Finkelman, R. B.; Palmer, C. A.; Wang, P. Quantification of the modes of occurrence of 42 elements in coal. *Int. J. Coal Geol.* **2018**, *185*, 138−160.
(37) Huggins, F. E.; Shah, N.; Huffman, G. P.; Kolker, A.; Crowley, S.; Palmer, C. A.; Finkelman, R. B. Mode of occurrence of chromium in four U.S. coals. *Fuel Process. Technol.* **2000**, *63*, 79−92.
(38) Ruppert, L. F.; Finkelman, R. B.; Boti, E.; Milosavljevic, M.; Kaluderovic, M.; Kolinovic, R. Significance of Ni- and Cr-rich minerals in the Kosovo lignite, Yugoslavia. *Geol. Soc. Am. Abstr.* **1991**, *23*, A144.
(39) Palmer & Filby. Distribution of trace elements in coal from the Powhatan No. 6 mine, Ohio. *Fuel* **1994**, *63*, 318−328.
(40) Kaback, D. S.; Runnells, D. D. Geochemistry of molybdenum in some stream sediments and waters. *Geochim. Cosmochim. Acta* **1980**, *44*, 447.
(41) Barling, J.; Anbar, A. D. D. Molybdenum isotope fractionation during adsorption by manganese oxides. *Earth Planet. Sci. Lett.* **2004**, *217*, 315.
(42) Chappaz, A.; Gobeil, C.; Tessier, A. Geochemical and anthropogenic enrichments of Mo in sediments from perennially oxic and seasonally anoxic lakes in Eastern Canada. *Geochim. Cosmochim. Acta* **2008**, *72*, 170.
(43) Goldberg, T.; Archer, C.; Vance, D.; Poulton, S. W. Mo isotope fractionation during adsorption to Fe (oxyhydr)oxides. *Geochim. Cosmochim. Acta* **2009**, *73*, 6502.
(44) Córdoba, P.; Ayora, C.; Querol, X. Evaluation of chemical stabilisatin methods of coal-petcoke fly ash to reduce the mobility of Mo and Ni against environmental concerns. *Ecotoxicol. Environ. Saf.* **2021**, *208*, 111488.
(45) Cho, K.; Wu, C. Control of Molybdenum Emission by Sorbents: Equilibrium Analysis. *J. Environ. Eng.* **2004**, *130*, 126.
(46) Koukouzas, N.; Ketikidis, C.; Itskos, G. Heavy metal characterization of CFB-derived coal fly ash. *Fuel Process. Technol.* **2011**, *92*, 441−446.
(47) Lu, Y.; Hu, S.; Liang, Z.; Zhu, M.; Wang, Z.; Wang, X.; Liang, Y.; Dang, Z.; Shi, Z. Incorporation of Pb (II) into hematite during ferrihydrite transformation. *Environ. Sci.: Nano* **2020**, *7*, 829.
(48) Zhou, C.; Liu, G.; Fang, T.; Wu, D.; Lam, P. K. S. Partitioning and transformation behavior of toxic elements during circulated fluidized bed combustion of coal gangue. *Fuel* **2014**, *135*, 1−8.
(49) Fu, B.; Liu, G.; Sun, M.; Hower, J. C.; Mian, M. M.; Wu, D.; Wang, R.; Hu, G. Emission and transformation behavior of minerals and hazardous trace elements (HTEs) during coal combustion in a circulating fluidized bed boiler. *Environ. Pollut.* **2018**, *242*, 1950−1960.
(50) Zhao, S.; Duan, Y.; Li, Y.; Liu, M.; Lu, J.; Ding, Y.; Gu, X.; Tao, J.; Du, M. Emission characteristic, and transformation mechanism of hazardous trace elements in a coal-fired power plant. *Fuel* **2020**, *214*, 597−606.
(51) Guo, B.; Nakama, S.; Tian, Q.; Pahlevi, N. D.; Hu, Z.; Sasaki, K. Suppression processes of anionic pollutants released from fly ash by various Ca additives. *J. Hazard. Mater.* **2019**, *371*, 474−483.
(52) Córdoba, P.; Lieberman, N. R.; Izquierdo, M.; Moreno, N.; Querol, X. Understanding the Impact of FGD Technologies on the Emissions of Key Pollutants in a co-Firing Power Plant. *J. Energy Inst.* **2020**, *93*, 518−532.

https://doi.org/10.1021/acsomega.1c07326
ACS Omega 2022, 7, 14697−14711